EFFECTS OF SOLAR GEOENGINEERING ON INDIAN MONSOON PRECIPITATION PATTERNS

Nina Grant

A SENIOR THESIS
PRESENTED TO THE FACULTY
OF PRINCETON UNIVERSITY
IN CANDIDACY FOR THE DEGREE
OF BACHELOR OF THE ARTS

RECOMMENDED FOR ACCEPTANCE
BY THE DEPARTMENT OF
GEOSCIENCES

Adviser: Gabriel Vecchi

April 16, 2021

This paper represents my own work in accordance with University regulations,

Abstract

The unlikelihood of staying below the Paris Climate goal of 1.5-2°C has led some to more seriously consider geoengineering to cool the planet as we continue cutting emissions. Injecting sulfate aerosols into the stratosphere cools the planet, mimicking volcanic eruptions, however, it is likely to alter global precipitation patterns. Few studies have been done on more regional scales to examine these changes in precipitation. This thesis investigates the precipitation changes in the Indian summer monsoon under four scenarios: double-CO_2, 1% reduction in solar radiation (offsets half of global warming), a northern hemisphere volcanic eruption, and a southern hemisphere eruption.

It is found that -1% solar radiation reduces Indian monsoon rainfall in a similar spatial pattern as double-CO_2 increases rainfall, implying solar geoengineering might moderate, rather than exacerbate precipitation changes in India. The asymmetric, volcanic eruptions lead to more complex spatial variations in precipitation changes, with some parts of India increasing in precipitation, while others decrease. It is also found that the Agung (SH) eruption leads to fractional precipitation changes of comparable magnitude to the double-CO_2 and -1% solar radiation experiments, indicating an uneven deployment of aerosols could be just as impactful as a doubling of CO_2. The mechanisms of these precipitation changes are partially explained by changes in moist static stability, energy convergence, and specific humidity, but leave large residuals, indicating other mechanisms like horizontal advection, eddies, and the subtropical jet stream may also be important in diagnosing the causes of precipitation changes associated with global warming and solar geoengineering.

Acknowledgements

I would like to thank everyone who helped me not only in this past year but in the three leading up to this. Thank you to all the instructors, mentors, and friends I have had along the way. Thank you to the GEO department for being so welcoming and supportive. I am so grateful that I found my way to and a place within this department.

A million and one thanks to my advisor, Gabriel Vecchi. I have been fortunate enough to work with him closely these past two years. Whether in the classroom or our weekly meetings, he always knows how to explain complex processes in a digestible manner. I was very nervous to begin independent research, but he has always reassured me throughout the process—reminding me no one starts off an expert or knows how to write scientific papers; I am only at the beginning of my journey. I also cannot thank you enough for not only being a great teacher but a great person as well. It has taken so much weight off of my shoulders knowing it is okay to ask simple questions, ask for re-explanations, or to have an "off" week. Having such a genuinely compassionate advisor has really helped me enjoy and embrace my thesis rather than be stressed or petrified. I am so grateful to have had the chance to work with you!

I would like to thank Jingru Sun for your help this year and last year. Thank you for taking the time to help me learn how to work with Linux systems and NetCDF files. I would not have been able to undertake this project without your guidance these past two years. Thank you to Wenchang Yang as well for helping me to understand both the technical and scientific facets of my thesis. Thank you for helping me troubleshoot my code and helping me understand the climate system models. Thank you to Larry Horowitz for agreeing to be my second-reader. A huge thank you to Tess Jacobson also for your insightful research and code which helped to frame my project. Lastly, thank you to Egemen Kolemen, whose class on geoengineering inspired this project.

Thank you to my friends and family for your support these last four years. I am especially grateful to my roommate, Asia, for providing me motivation and accountability this semester as we tackled our theses together. I could have not have made it through this past tumultuous year without the love and support of my family either. Thank you for sharing bandwidth with me back home and helping me navigate being a student while living at home during a pandemic.

Contents

List of Figures

List of Tables

Introduction

Disastrous effects of global warming are becoming harder to avoid. The Paris Agreement set goals to contain this warming to 1.5-2°C. However, most countries have been slow to make impactful reductions of their emissions which makes the odds of reaching the Paris Agreement goals far slimmer or even impossible (Zhou et al., 2021). On February 28, 2021, an interim update report commissioned by the UNFCCC found that current pledges (by parties compromising 30% of global GHG emissions) on average will reduce emissions by 0.5% below 2010 levels by 2030. However, IPCC Reports suggest that reductions of 45% will be needed by 2030 to reach the 1.5°C target and 25% to avoid >2°C (UNFCCC, 2021). This has led some to consider more seriously the use of solar geoengineering (SG) or solar radiation management (SRM)—intentionally altering the amount of solar radiation that reaches the Earth's surface—as a temporary band-aid solution to allow mankind more time to reduce greenhouse gas emissions. One of the most popular schemes mimics the effects of volcanic eruptions by spraying sulfate aerosols into the stratosphere to reflect solar radiation and cool the planet. However, there are a number of possible side effects that could come from cooling the Earth in this manner (Robock, 2008). One of the biggest problems is a likely disturbance of precipitation patterns. The South Asian Monsoon impacts the lives of over a billion people in the Indian sub-continent and surrounding areas. Disruptions in precipitation patterns (magnitude, timing, duration, and location) could be catastrophic to agricultural practices in a country where agriculture accounts for 16% of the GDP and is based primarily on rainfall, not irrigation (Sahany et al., 2018). Changes in precipitation also lead to flooding and droughts, which again are particularly impactful to a nation in which not all localities have the infrastructure to withstand floods or rely heavily on rainwater for drinking water.

India Under Global Warming

In the 5th assessment report by the IPCC, the monsoons of South Asia are expected to change dramatically under the current warming scenario. Chapter 24 notes that all CMIP5 models predict increases in mean precipitation as well as heavy precipitation during the Indian monsoon (Hijioka et al., 2014). Chapter 14 Section 8.11

reports average seasonal rainfall has been decreasing during the South Asian monsoon but heavy precipitation events have been rising (Christensen et al., 2014). CMIP5 models show greater changes in the summer than winter monsoon precipitation, although there is more variability among the models on how the winter monsoon changes. Both CMIP3 and CMPI5 models have been poor in simulating monsoon breaks and how they will change, but it seems the number of monsoon break days has been and may continue to increase. Furthermore, they observe further sub-regional variations in precipitation across model runs.

Sahany et al. (2018) delve deeper into the subregional variations in precipitation. Using observational data from 1901 to 2013, they find the regions with the most total rainfall and seasonality are the Western Ghats, Central India, Northeast India, and over the Indo-Gangetic plains (Northern Plains) (all shown in the map below), but they also report a significant decrease in the seasonality and rainfall in parts of central India, the Indo-Gangetic plains, and parts of Western Ghats over the time series investigated.

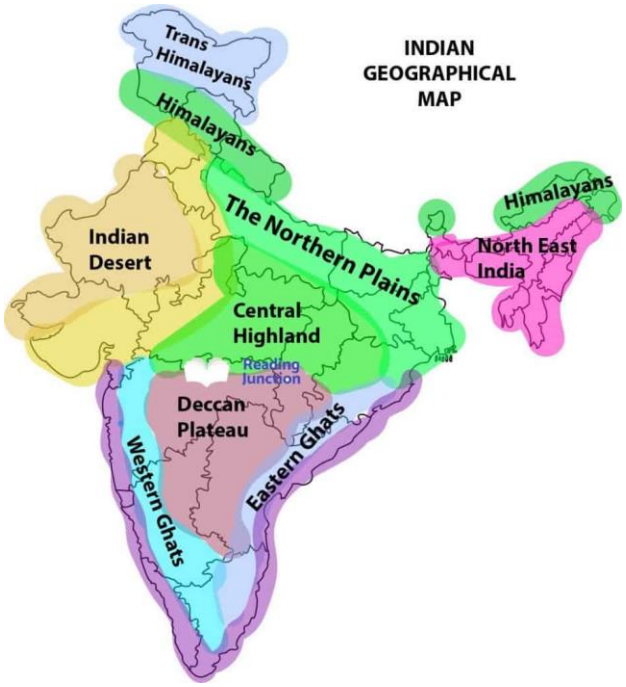

Figure 1*| Map of India split by geographical regions by Reading Junction. Sahany et al (2014) find strong rainfall and seasonality over the Western Ghats, Central India (Central Highland), North East India, and the Indo-Gangetic plains (Northern Plains).*

Impacts of Solar Geoengineering (SG) and Volcanoes

A number of studies have also been conducted on the hydrological impact of solar geoengineering. In a 2019 publication, Bal et al. find, in a 4xCO2 scenario, precipitation

increases across most of the globe, but the duration of peak precipitation changes regionally. Using relative entropy, seasonality index, duration of the peak rainy season and timing of the peak rainy season as metrics for hydrological response, they find solar geoengineering is able to reduce the global increase in precipitation and restore timing of the precipitation, but it does not restore changes in the seasonality index in places like northern South America, the Arabian Sea, and southern Africa.

Volcanic eruptions are often used as substitutes for solar geoengineering experiments. In Yang et al. (2019), historic volcanic eruptions are modeled to observe the global climate hydrological response, specifically how global temperatures, precipitation, and tropical cyclone (TC) activity change in response to three volcanic eruptions. When a large eruption occurs in the northern or southern hemisphere, mean surface temperatures all respond similarly to an equatorial eruption. However, the precipitation and TC activity response is found to be larger for the asymmetric eruptions, due in part to a shifting of the Intertropical Convergence Zone (ITCZ). It is also noted that the magnitude of the eruption is not proportional to the impact. While the Pinatubo eruption was much greater, small eruptions, if asymmetric, can lead to greater regional climate changes.

Jacobson et al. (2020) also consider the meridional structure of volcanic eruptions and its effect on precipitation patterns, but taking a regional focus. The Sahel region in Africa is a semi-arid region, making it highly susceptible to changes in rainfall. Using GFDL's FLOR model and NCAR's CESM 1.1 model to simulate 46 volcanic eruptions, they find eruptions and cooling in the Northern Hemisphere lead to a drying of the Sahel, while southern cooling leads to a wetter Sahel. The two models, however, show a difference in the timing of the rainfall, with the FLOR model showing consistent timing between the northern, southern, and equatorial eruptions but the CESM model resulting in temporal differences in the rainy season among the eruptions

There is a general consensus that sulfate injections would alter precipitation patterns, making some areas wetter and others drier. Jacobson et al. (2020) and Yang et al. (2019), while investigating the meridional structure of eruptions, find the location of the injection/eruption matters. Eruptions in the Northern Hemisphere (NH) led to a drier NH but wetter Southern Hemisphere (SH), eruptions in the SH led to a drier SH but

wetter NH, and eruptions on the equator led to more global cooling but less local changes in precipitation.

Irvine et al. (2019) investigates a middle ground where sulfate injections are used (symmetrically) to counteract only half of forcing from GHGs. In a global study, they analyze locations where local climate changes are minimized or exacerbated by full-scale SRM to gage whether using SRM to only halve the warming reduces the severity of the changes. They find for most of the globe a half-SRM solution minimizes the effects seen under a double CO_2 scenario. However, it is important to note, there are a handful of regions, like western South America, southern Africa, or the eastern most part of Brazil, that show exacerbated precipitation changes in some percentage of the GEOMIP models (shown in Fig 2 below taken from Fig 3 of Irvine et al. 2019). They also find above halving the warming, climate risks seem to increase such that SG is more harmful than beneficial. While they do not conduct a thorough investigation of the optimal solar radiation reduction needed, this does at least suggest that it is possible to cool the Earth without any major climate disruptions if SRM is optimized.

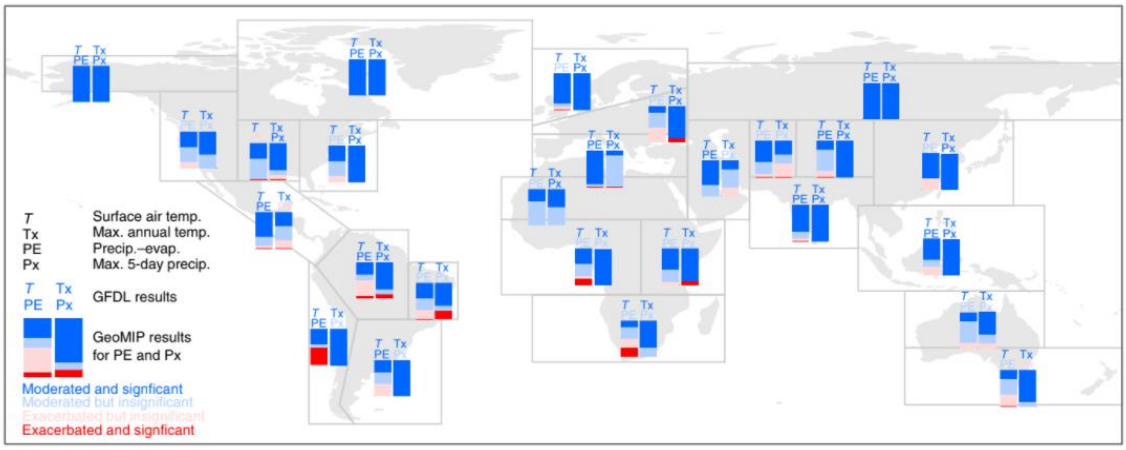

Figure 2 | Figure 3 from Irvine et al. 2019, *"**Regional distribution of where half-SG moderates or exacerbates the absolute magnitude of 2×CO2 anomalies in HiFLOR (for T, Tx, PE and Px) and the GeoMIP ensemble (PE and Px).** Regions where half-SG moderates (blue) or exacerbates (red) the absolute magnitude of the 2×CO2 climate anomalies relative to control are illustrated. Statistically significant results are indicated with bold colours whereas insignificant results are shown with pale colours (see Methods). The results for the GeoMIP models are shown for precipitation–evaporation (PE, left-column) and Px (right-column) with the columns coloured to indicate the fraction of GeoMIP models with each result. All GeoMIP models show a statistically significant reduction in T and Tx in all regions (not shown)."*

Understanding Precipitation Change Mechanisms

Rainfall is fundamentally controlled by the conservation of mass and energy. Rainfall is determined by the amount of moisture in the air and the vertical motion of a

parcel of air. This relationship is shown in the equation below, where P is precipitation, q is specific humidity (a product of relative humidity (rh) and saturated specific humidity (q^*)), and ω is ascent.

$$\frac{dP}{P} = \frac{dq}{q} + \frac{d\omega}{\omega}$$

$$q = rh * q^*$$

Moisture can increase by having more evaporation than precipitation or by bringing in moist air horizontally. Evaporation alone usually does not increase enough to lead to large changes in precipitation; instead, horizontal transport of moist air is usually responsible. Vertical motion or ascent is also required for precipitation. Air is condensed as it moves up the troposphere and adiabatically cooled, such that even a parcel of air which would not have been saturated at the surface can reach saturation level as it rises and cools. Therefore, increasing vertical motion can also increase precipitation. One of the fundamental research questions of this thesis is teasing out the mechanisms by which Indian precipitation changes in each experiment, determining whether precipitation changes are dominated largely by dynamic (vertical or horizontal motion) or thermodynamic (moisture) changes.

However, considering mass balance alone can become a problem as ascent can be driven by horizontal convergence or convergence can be driven by ascent. Adding an energy balance helps to break this loop as it constrains the ascent term. Moist static energy (MSE) is the sum of the latent, sensible, and gravitational energies in a parcel of air. Static stability relates to buoyancy and considers the gravitational resistance applied to a parcel of air as it moves vertically and can be approximated by finding the vertical gradient in MSE (Seth et al., 2013). Chou and Neelin (2003) argue that ascent is governed by stability and energy convergence as shown in the equation below, where ω is ascent, S is stability, and Q is energy convergence.

$$\frac{d\omega}{\omega} + \frac{dS}{S} = \frac{dQ}{Q}$$

Assuming relative humidity is constant, we can combine the mass and energy balances by the ascent term as follows such that increases in precipitation are due to increases in specific humidity, increases in energy convergence, or decreases in stability (plus an error term).

$$\frac{dP}{P} = \frac{dq}{q} + \frac{d\omega}{\omega}$$

$$\frac{d\omega}{\omega} = \frac{dQ}{Q} - \frac{dS}{S}$$

$$\frac{dP}{P} = \frac{dq}{q} + \frac{dQ}{Q} - \frac{dS}{S} + \epsilon$$

Several predictions have been made about how these quantities may change with global warming. Held and Soden (2006) argue that while moisture increases with warming according to Clausius-Clapeyron, precipitation should increase at a slower rate closer to 2% K^{-1} and relate to changes in radiative flux. Since precipitation is expected to increase more slowly than moisture in a warming planet, to balance the above equations, circulation must compensate by slowing down, or in other words water vapor must have a longer residence time in the troposphere (Held and Soden, 2006). Knutson and Manabe (1995) alternatively argue that the subsidence rate weakens as a result of dry static stability increasing faster than radiative cooling in the troposphere.

In the volcanic experiments done by Jacobson et al. (2020), it was found that stability increased slightly in the African Sahel region after three different volcanic eruptions—Pinatubo (symmetric), Agung (in the Southern Hemisphere), and St. Maria (in the Northern Hemisphere). This, however, is inconsistent with what Chou and Neelin (2003) predict should happen. The difference is attributed to the horizontal advection during the monsoon season which is not accounted for in the MSE framework. Jacobson et al. (2020), rather than moist static stability, instead focus on changes in radiative and turbulent fluxes to analyze changes in the West African monsoon.

Given current knowledge of global hydrological changes due to global warming, SRM, and asymmetric aerosol forcings, it is expected that an asymmetric forcing will lead to greater perturbations in the South Asian monsoon precipitation pattern than even the CO2x2 scenario. I also hypothesize that the CO2x2 and -1% experiments will largely affect identical areas within India while the asymmetric experiments will shift the location of precipitation anomalies. Lastly, I predict local changes in mass and energy will help explain the precipitation changes observed.

Methods

The data analyzed in this study come from global climate models utilized in Yang et al. (2019) and Irvine et al. (2020). Both studies rely on the FLOR model (Vecchi et al., 2014). The Forecast-oriented Low Ocean Resolution (FLOR) model, developed at the Geophysical Fluid Dynamics Laboratory (GFDL), is a descendant of the CM2.5 model (Delworth et al., 2012) and CM2.1 model (Delworth et al., 2006). Using the same low horizontal resolution of CM2.1 for ocean and sea ice components (approximately 1°) but higher horizontal and vertical resolution in the atmosphere and land (50 km compared to 200 km in CM2.1), FLOR is able to more efficiently model regional climatic extremes like tropical cyclones (Vecchi et al., 2014; Yang et al., 2019), droughts (Delworth et al., 2015), extratropical storms (Yang et al., 2015), and temperature and precipitation changes over land (Jia et al., 2015; Jacobson et al., 2020).

Past studies, like Irvine et al. (2019) and Yang et al. (2019), have primarily focused on global or zonal patterns. This study will take a more focused approach on one country, India. Seasonal Indian monsoon behaviors (June-July-August) are analyzed in four experiments: CO_2x2, -1% solar radiation, northern hemisphere eruption (St. Maria), and a southern hemisphere eruption (Agung). The control experiment was run using preindustrial (1860) conditions for 1000 years. Reducing solar radiation by 1% is used to offset half of the warming that would come from doubling atmospheric CO_2 (Irvine et al., 2019). The volcanic experiments are run over a period of five years with 30 ensembles. The Agung eruption of 1963 injected 17 Tg of sulfate into the atmosphere and 4 Tg for the St. Maria eruption of 1902 (Robock, 2015).

To illustrate and interpret the behavior of the South Asian Monsoon and corresponding spatial and temporal changes, this study relies mostly on changes in total precipitation, energy, and moisture. This paper relies heavily on the moist static energy framework to understand changes in precipitation over India. Precipitation, humidity, convective mass flux, energy convergence, and moist static stability are used as metrics in diagnosing the changes in precipitation in the region.

As discussed in the introduction, in a warming world, precipitation is not expected to increase as rapidly as atmospheric moisture. This leads to changes in atmospheric

circulation which can be quantified by calculating changes in convective mass flux (Held and Soden, 2006). Vecchi and Soden (2007) use the following equation, where M'_c is the estimated (not precise) convective mass flux, P is precipitation, T is temperature, and the coefficient 0.07 comes from the Clausius-Clapeyron relation.

$$\frac{\Delta M'_C}{M'_C} = \frac{\Delta P}{P} - 0.07\Delta T$$

To isolate the mechanisms behind the changes in precipitation, moist static energy is used as a framework. Moist static energy, as explained in the introduction, depends on temperature, humidity, latent heat, and potential energy. The equation is shown below in which C_p is the specific heat capacity of the atmosphere, T is the temperature of the air, g is the gravitational constant, Z is the height, L is the latent heat of condensation, and q is the specific humidity. Moist static stability, ΔMSE or S, is calculated as the difference between MSE in the upper troposphere and the lower. This paper, like Jacobson et al. (2020) uses the pressure levels of 200 and 850 mb for the calculation.

$$MSE = C_pT + gZ + Lq$$

$$S = \Delta MSE = MSE_{200\,mb} - MSE_{850\,mb}$$

As explained in the introduction, the change in precipitation is broken down into its components. Substituting ascent, ω, the change in precipitation is calculated as:

$$\frac{dP}{P} = \frac{dq}{q} + \frac{dQ}{Q} - \frac{dS}{S} + \epsilon$$

The energy term, Q, in this paper is the energy convergence into the troposphere, ΔF, and is defined as the sum of any latent heat (LH), sensible heat (SH), and long/shortwave fluxes at the top of the atmosphere (TOA) and surface (combined as net radiation flux, *Net*). Flux outputs from the model are defined as positive in the upward direction. Therefore, the energy into a column of air is the net surface fluxes minus the TOA fluxes, as shown in the equation below.

$$Q = \Delta F = Net_{Sfc} + LH_{sfc} + SH_{sfc} - Net_{TOA}$$

Most anomaly calculations in this paper are converted to fractional changes to better capture the overall magnitude of the change and to more easily compare the relative magnitude of the changes between metrics (precipitation, humidity, MSE, energy convergence, etc.). The fractional changes are calculated as follows:

$$\frac{Experiment\ -\ Control}{Experiment\ +\ Control}$$

Correlation analyses are also utilized to determine differences in the distribution of precipitation anomalies. Monsoon precipitation is responsible for most of the annual precipitation in India and two regions in particular—the Western Ghats (WG) and the Ganges-Mahanadi Basin (GB)—account for most of the interannual variance (Vecchi and Harrison, 2004). These two regions defined as 72.5°E-77.5°E, 7.5°N-20°N (WG) and 77.5°E-87.5°E, 20°N-27.5°N (GB) are expected to show high variability in the experiments as well. However, spatial correlation analyses are computed to determine whether the WG and GB regions do in fact remain the primary source of precipitation variation in India. Spatial pattern correlations (calculated by taking the Pearson correlation of the gridded data flattened into a 1D array) are also utilized to determine whether the CO_2x2, -1%, Agung, and St. Maria experiments affect only the magnitude of change or the spatial distribution as well.

Results

Figure 3 shows the change in precipitation over India under the four experiments. The boxes highlight the WG and GB regions which are expected to show the most change. Represented as a fractional change, as explained in the Methods section, we see largely opposite precipitation responses in the two non-volcanic experiments. In the double CO_2 experiment, precipitation increases minimally (below 6%) in half of the country during monsoon season. However, in the southern part of India (including the Deccan Plateau and the WG, especially in the northern part) and the Himalayas (near 30°N), there are more substantial changes, between 6% and 24% increases in precipitation. In the -1% SR experiment, we see overall drying in India during the monsoon months, with one exception in the Thar Desert which sees a slight increase in precipitation. During the monsoon season, the locations of the major precipitation changes are largely similar between the $2xCO_2$ and -1% SR experiments (with smaller changes in the central highlands, northern plains, and northeastern India and greater changes in the southeast and Himalayas), though the magnitude of change is larger in the former.

The volcanic experiments are far less uniform. In the St. Maria (NH) eruption, there is mostly a drying over India (~6% less precipitation), but there are a number of locations which increase in precipitation, namely the southern tip of the country (>12%), parts of the Thar Desert (>18%) and parts of Northeastern India. The Agung (SH) eruption shows a more uniform precipitation response, with almost the entire country showing an increase in precipitation (especially in the Thar Desert), with the exception of small regions in the eastern part of the Northern Plains. While most of the country sees an increase below 12% in precipitation, locations in the Thar Desert increase anywhere from 18% to over 45%.

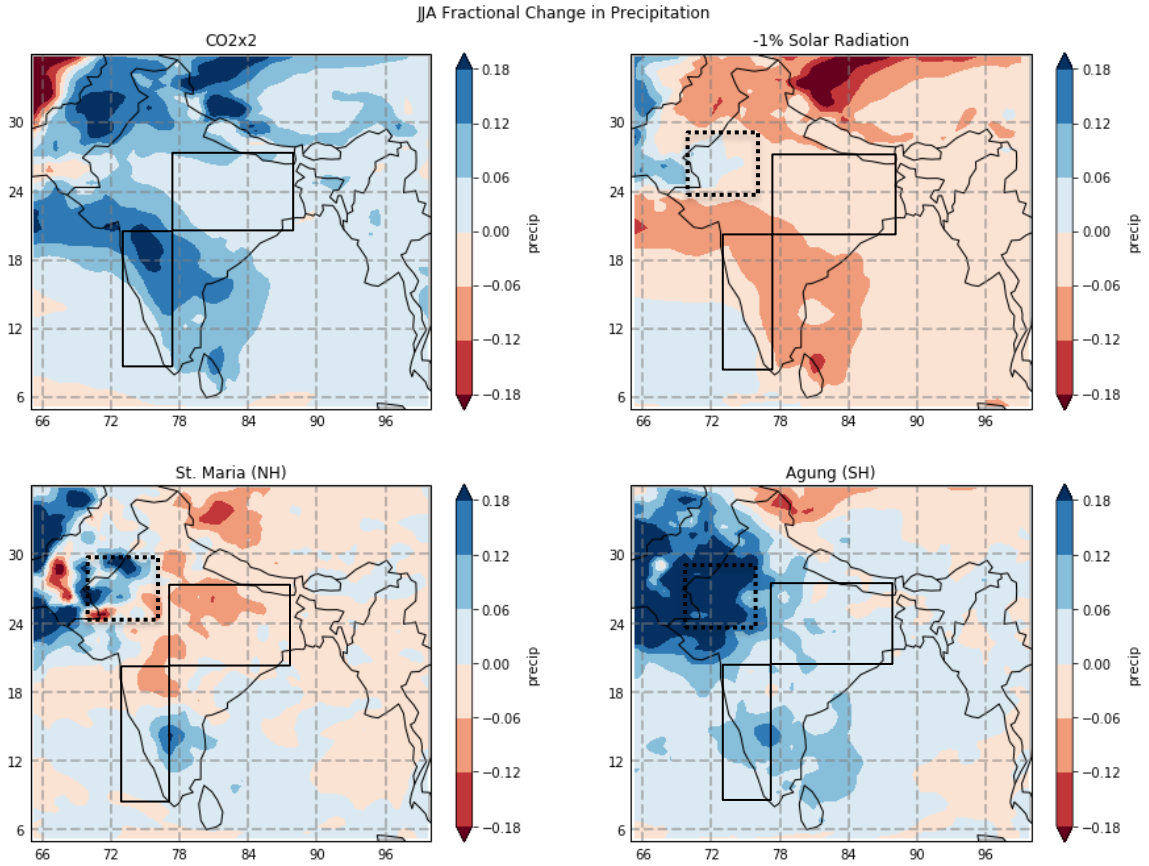

***Figure 3** | Average JJA precipitation anomalies expressed as fractional changes. The solid black boxes show the WG and GB regions. The dashed black shows the wet anomalies in the Thar Desert.*

The modeled changes in specific humidity are shown in Figure 4 below. Rather than the largest changes occurring in the southern half of India as seen with precipitation, we see some of the smallest changes in the southern tip and northeastern corners of India. These regions moisten by about 6% in the CO2x2 experiment but dry by about 3.75% in the -1% SR experiment. For specific humidity, the greatest increases are in the central and northwestern parts of India, with most of the region seeing a 10% moistening for CO2x2 and 6% drying for -1% SR. The greatest changes in moisture occurred over the Thar Desert in both experiments, drying by around 9% with -1%SR but moistening by ~14% with double CO_2.

The volcanic experiments differ in magnitude and uniformity again. In the St. Maria (NH) eruption, there is very slight drying across the country (below 2%, with large parts below 1%, with the exception of the WG/southern tip which sees a moistening of 0.5%). The Agung (SH) eruption is largely the opposite, with drying in the southern tip

and northeastern India (below 1%) and moistening below 3% in most of the rest of the country. In all experiments, the largest fractional changes occur in the northwest over the Thar Desert and the beginnings of the Himalayas and the smallest changes over the southern and northeastern segments.

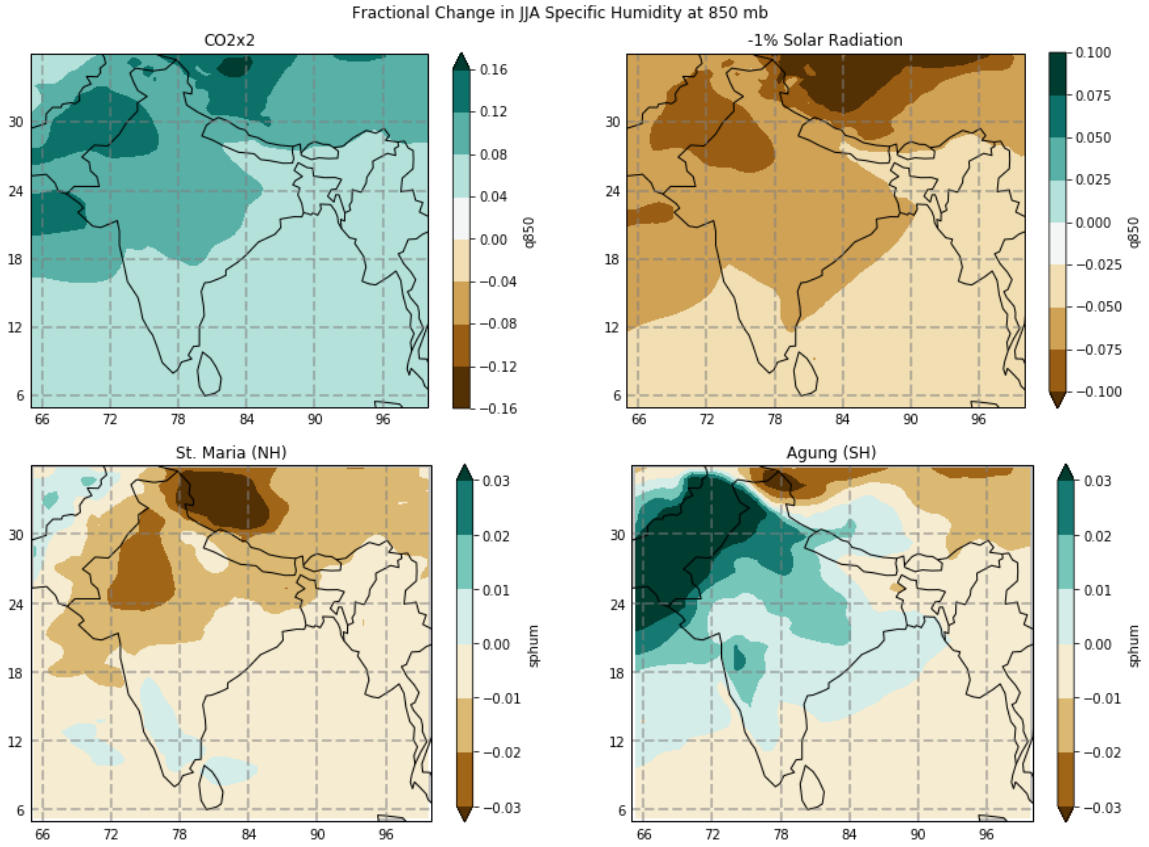

Figure 4 *| Fractional Changes in Specific Humidity (at 850 mb)*

The changes in the tropospheric energy convergence (ΔF or Q) are shown in Figure 5 below. A positive flux change means more net energy flux into the troposphere and a negative flux indicates more outward flux. Northern India sees, for the most part, minimally decreased energy convergence in -1% SR (<-2%); the WG have concentrated anomalies above a 6% decrease and increase in convergence, and in most of Southern India (over the Deccan Plateau and Eastern Ghats) there is a minimal increase in convergence (<2%). The CO2x2 model shows similar spatial layout with greater magnitude. Northern India (especially over the desert) increases in convergence (<2% in the Plains and >6% in parts of the desert). Southern India overall sees a decrease in convergence, especially over the Deccan Plateau (-4%), while the WG have clumps of

strong anomalous increases in convergence (>6%). The Himalayas—for both—show the greatest perturbations.

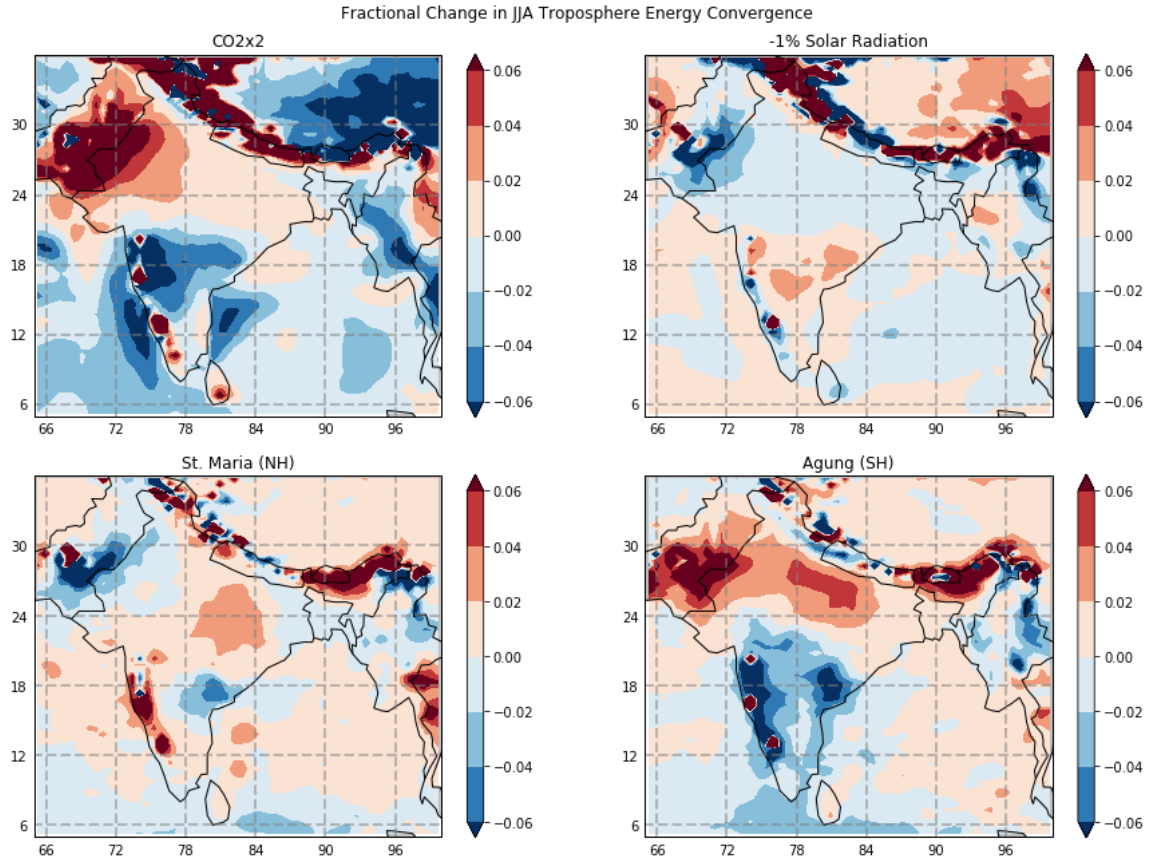

Figure 5 *| Fractional Change in JJA Atmospheric Energy Convergence. Calculated as the sum of the surface fluxes (LW, SW, SH, and LH) minus the TOA fluxes for all sky conditions. Positive fluxes are into the troposphere.*

For the volcanic experiments, we again see much less uniformity across the country, yet the magnitudes are comparable to the non-volcanic experiments. The St. Maria (NH) eruption shows decreased convergence in the Eastern Ghats (-4%) and the Thar Desert (<2%) but increased convergence in the Central and Northern Plains (3%) and the WG (>6%). The Agung (SH) eruption shows increased convergence in the northern half of the country (~3%) but decreases in the southern half—again with a more significant decrease (~7%) in the WG. There are even 3 clumps of increased convergence >6% embedded in the WG. The Himalayas again show large changes >6%—this time concentrated in the northeast.

Following the frameworks discussed in the introduction, convective mass flux and moist static energy are used to isolate the responsible mechanisms for the changes in precipitation. Figure 6 shows the fractional changes convective mass flux across the four

experiments during the monsoon season. We see the CO2x2 experiment experiences an increase in the estimated convective mass flux over the southern half of the country (especially over the WG with increases around 30%) as well as the Himalayas and Northern plains (<15%). Most of the Central Highlands, Thar Desert, and NE India however show slight decreases in M_C (<10%). The -1% SR experiment sees a similar spatial distribution of the opposite sign. M_C decreases in the southern half of the country and the Himalayas (<10%), but increases over the Thar Desert (~15%), parts of the Central Highlands and NE India (<10%). In the volcanic experiments, the St. Maria eruption leads to a decrease in M_C over most of the country (below 20%) but a marked increase in the southern tip (~30%) and the parts of the Thar Desert (~50%). In the Agung (SH) eruption, virtually the entire country sees an increase in M_c but the same regions as the St. Maria eruption show a more significant increase. The southern tip increases by a similar amount, around 30%, but the Indian Desert sees a wider reaching and higher magnitude increase in M_C, with a large extent showing increases above 60%.

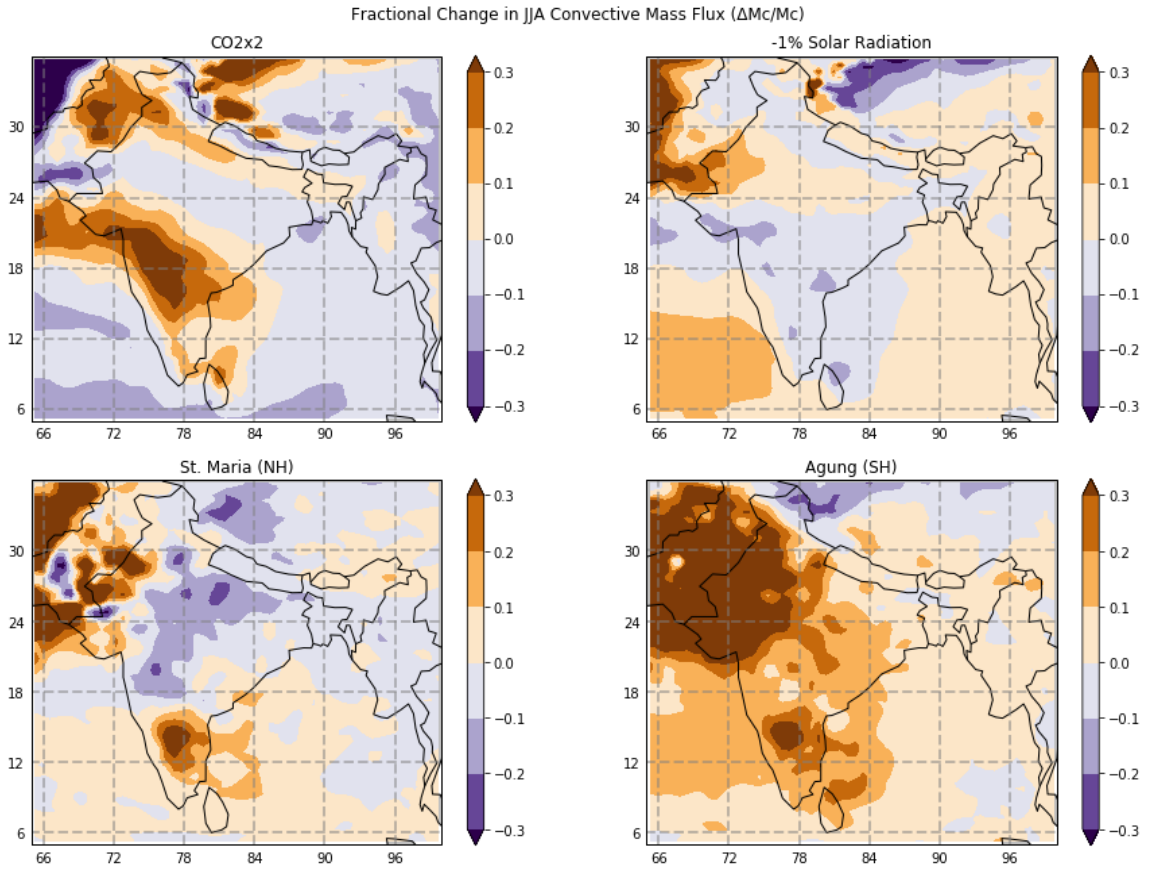

***Figure 6** | Fractional change in JJA convective mass flux. Calculated as dMC'/MC' = dP/P - 0.07dT, where P is precipitation, T is temperature, and MC' is the estimated convective mass flux.*

Following the approach taken in Jacobson et al. (2020) and described in the Methods section, the moist static stability is represented as a fractional change. Moist static stability weakens over most of India in the CO2x2 experiment—except for the southern tip which increases slightly (<3%), meanwhile ΔMSE increases in the -1% SR experiment by about half the magnitude. In both non-volcanic experiments, ΔMSE has the most pronounced changes concentrated in the northern and central parts of India, decreasing by more than 12% with CO2x2 and increasing by about 5% with -1% SR. Stability does not significantly change however for the volcanic experiments. For the St. Maria (NH) eruption ΔMSE decreases slightly (~0.2%) for most of the country but increases somewhat over the WG and southern part of India (<0.2%). For the Agung (SH) eruption, ΔMSE slightly increases over most of the country by <0.2% (with somewhat more pronounced increases in the northwestern Himalayas) and decreases by <0.2% in the Eastern Ghats and parts of NE India.

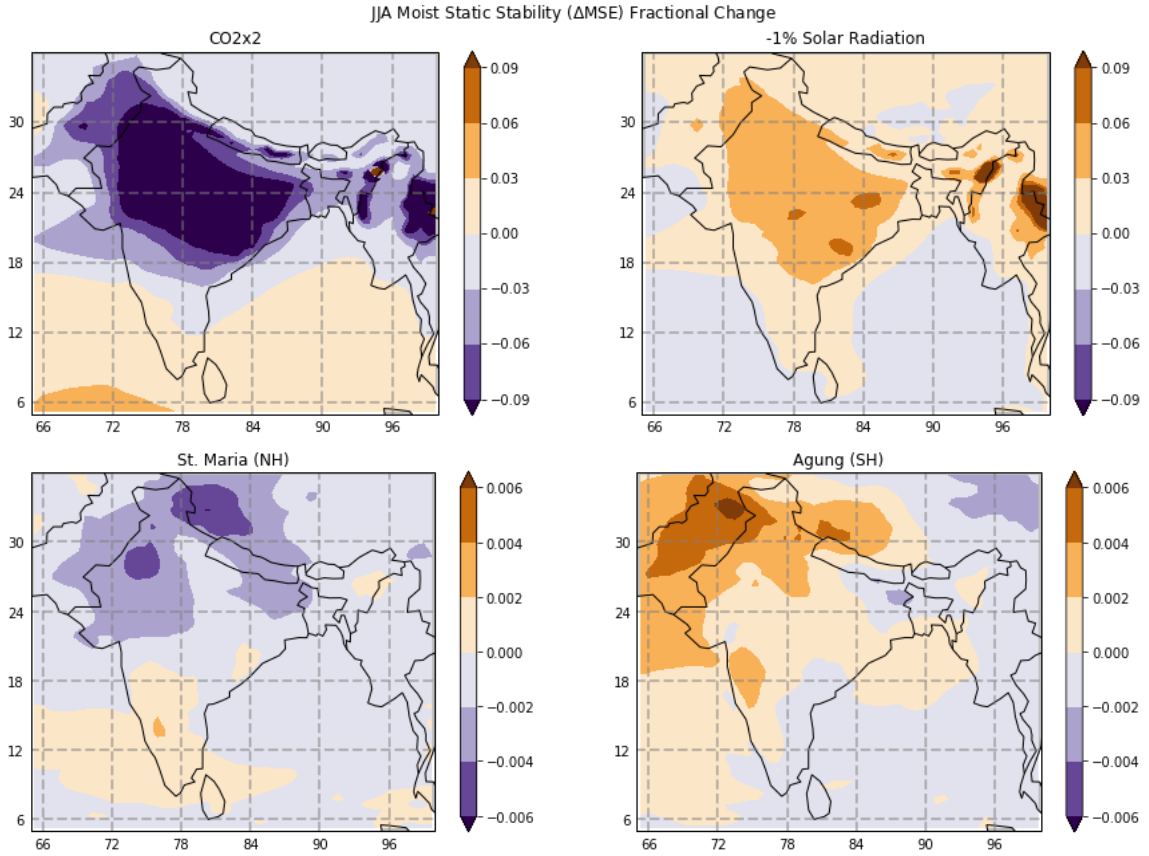

***Figure 7** | Fractional Change in Moist Static Stability (ΔMSE or dS). Calculated using the vertical gradient in MSE between 200 mb and 850 mb.*

To determine how similar the experiment anomalies were in spatial distribution, correlation coefficients were calculated and are summarized in Table 1 below. The CO2x2 and -1%SR experiments are strongly, negatively correlated in spatial distribution for precipitation, specific humidity, and convective mass flux but weakly, negatively correlated in stability fractional changes. There is no correlation in the fractional changes in energy convergence between the two non-volcanic experiments. The St. Maria (NH) and Agung (SH) eruptions are strongly, positively correlated in precipitation and convective mass flux fractional changes but have no correlation in specific humidity and energy convergence changes. There is a moderately weak negative correlation in their stability changes for the eruptions.

	dP/P	**dq/q**	**dQ/Q**	**dM_c/M_c**	**dS/S**
CO2x2 v. -1% SR	-0.768	-0.906	0.011	-0.691	-0.209
NH v. SH	0.696	0.061	0.030	0.690	-0.335

***Table 1** | Spatial correlation coefficients. Row 1 shows the Pearson correlations between the CO2x2 and -1%SR experiments for each map made. Row 2 shows the correlations for the NH and SH eruption maps.*

Correlation coefficients were also calculated to determine how well the precipitation anomaly distribution in each experiment aligns with the other metric anomalies, summarized in Table 2 below. For the CO2x2, -1%, and St. Maria experiments, precipitation is moderately correlated (positive) to fractional changes in specific humidity, while the Agung experiment has a strong positive correlation between the precipitation and specific humidity changes. The changes in energy convergence have no spatial correlation to the precipitation changes for all four experiments. There are strong positive correlations between the precipitation and convective mass flux changes for all four experiments. The CO2x2 experiment shows no correlation between the spatial distribution of the precipitation changes and the moist static stability changes. The -1% SR/St. Maria experiments show very weak negative/positive spatial correlations for precipitation and stability, while the Agung experiment is the only one to show a moderate, positive correlation between the two metrics.

	dq/q	dQ/Q	dM_c/M_c	dS/S
CO2x2	0.532	0.087	0.944	-0.007
-1% SR	0.531	0.039	0.872	-0.159
St. Maria (NH)	0.403	-0.004	0.792	0.237
Agung (SH)	0.729	0.033	0.935	0.522

***Table 2** | Spatial precipitation correlation coefficients. Row 1 shows the correlation between the CO2x2 precipitation fractional changes and the fractional changes of the other metrics. Row 2 shows the precipitation v. metric(x) correlation for the -1% SR experiment.*

Discussion

Three predictions were made in the Introduction. The first was that the CO2x2 and -1% experiments would largely affect the same areas, but that the volcanic experiments would vary in spatial distributions. This prediction seems to be true for the fractional changes in precipitation. The CO2x2 and -1% SR experiments had a spatial correlation of -0.768, indicating that, for the most part, the same regions were affected by both experiments. One of the main points of difference was that the Thar Desert saw an increase in precipitation for both experiments rather than a drying for the -1%SR experiment. The changes in specific humidity and convective mass flux were also strongly correlated (-0.906 and -0.691, respectively). However, the changes in moist static stability were weakly correlated, indicating the two experiments impacted stability differently across the country.

The volcanic experiments, as predicted, varied in spatial distribution from the non-volcanic experiments. The asymmetric eruptions were weakly correlated to the CO2x2 and -1% SR experiments in precipitation changes yielding the following correlations: CO2x2 & NH = -0.312, CO2x2 & SH = -0.003, -1%SR & NH = 0.376, and -1%SR & SH = 0.322. This indicates that the asymmetric forcing due to the asymmetric eruptions is important in the spatial distribution of precipitation changes even within India. Furthermore, the spatial distributions also varied slightly between the two asymmetric eruptions, with a spatial precipitation correlation of 0.696. This value is rather high and similar to that of the non-volcanic experiments (-0.768); however, the sign is not flipped as was predicted. The St. Maria (NH) eruption should have led to an overall drying over India while the Agung (SH) eruption leads to an overall increase in precipitation. Part of this discrepancy could be due to the overall magnitude of the eruptions. As stated in the Methods section, the Agung eruption emitted 17 Tg of sulfate into the atmosphere compared to only 4 Tg with the St. Maria eruption. This could explain why there are stronger and more uniform changes with the Agung eruption compared to the weaker St. Maria one.

The next prediction was that the asymmetric volcanic forcings would lead to precipitation perturbations even greater than the CO2x2 or -1%SR experiments. Shown in

Figure 8 below, the fractional change in precipitation over all of India (defined as 72.5°E-85°E, 7.5°N-30°N) is greatest for the CO2x2 experiment, followed closely behind by Agung (SH), then -1% SR, then St. Maria (NH) with the smallest change (very close to 0%). This somewhat aligns with the prediction, in that the SH eruption, even over a brief 5-year period could approximate the magnitude of change seen by the non-volcanic runs.

One of the points of difference from the predictions is the location of the precipitation, convective mass flux, stability, humidity, and energy convergence changes. Firstly, while the WG and GB regions have been shown to have a high mean and variance in rainfall (Vecchi & Harrison, 2004), they are not the primary areas of fractional precipitation change in these experiments. Instead, the southern half of India (which encompasses the WG) and the Northwest Himalayan regions saw the greatest fractional change in precipitation. For this reason, rather than using WG and GB as the two primary regions of focus, further analysis of India will be done by splitting the country into the Northern and Southern half along 21°N, as shown in Figure 8 below. By splitting the changes into North and South, we see that the NH eruption has slightly stronger precipitation changes in the North (drying) that are compensated by opposing (moistening) changes in the South. However, the magnitudes for both North and South are still much smaller (<3%) than the other experiments (>5%). This asymmetry in precipitation change is also seen in the Agung experiment, while the non-volcanic experiment changes are more symmetric (though for both, South India sees a slightly larger fractional change).

The second spatial difference of note is that the regions of greatest fractional change in precipitation do not align with the other metrics calculated. As shown in Table 2, specific humidity, for instance, does not increase in the same areas as precipitation does for three of the four experiments (CO2x2 – 0.532, -1%SR – 0.531, St. Maria (NH) – 0.403, Agung (SH) – 0.729). This could be due to the fact that the anomalies are characterized as fractional instead of absolute changes. The WG and Northeastern India are already moist places. Humidity changes should be largest in locations that are either drier to begin with or not close enough to the ocean (which has essentially limitless water that can evaporate) to have more consistent humidity. All four experiments in fact show greater fractional changes in specific humidity in the North (further from the ocean and home to the Indian Desert) compared to the South (bordered by the ocean).

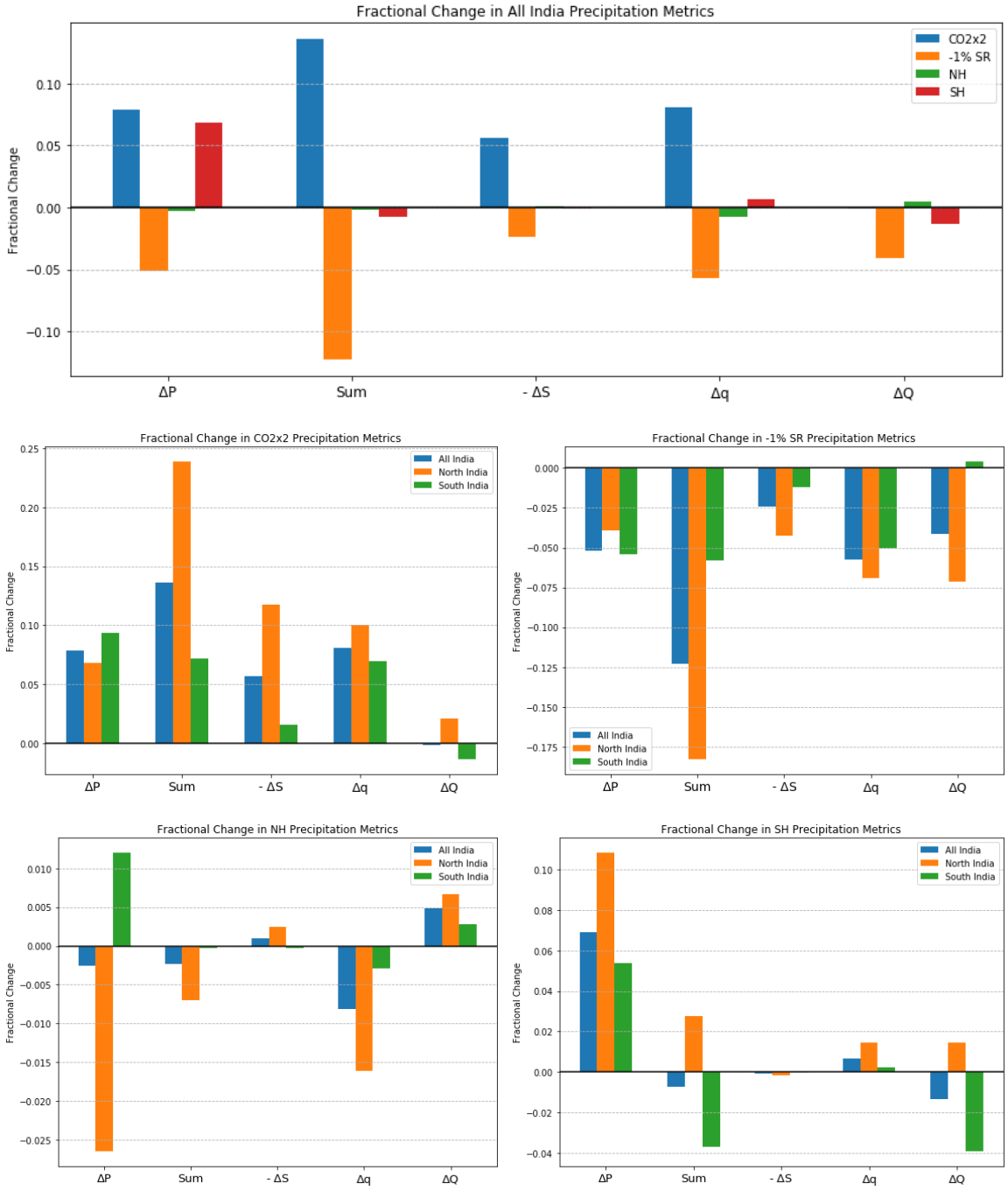

Figure 8 *Summary of the fractional changes in precipitation metrics. All India is defined as 72.5°E-85°E, 7.5°N-30°N. North India is defined as 72°E-84°E, 21°N-30°N. South India is defined as 72.5°E-81°E, 7.5°N-21°N. The variable Sum adds the fractional changes in instability (-ΔS), specific humidity (Δq), and energy convergence (ΔQ).*

Moist static stability changes also do not align with the precipitation anomalies for most of the four experiments (CO2x2 – -0.007, -1%SR – -0.159, St. Maria (NH) – 0.237, Agung (SH) – 0.522). This could in part be due to the difference in specific humidity changes, however it was also predicted that moist static stability may not prove helpful, at

least for the volcanic experiments, as Jacobson et al. (2020) found it to be inconsistent with predictions from Chou and Neelin (2003). Figure 7 showed the changes in stability were concentrated over the central/northern parts of India rather than the southwestern parts where precipitation changed by the greatest ratio.

Convective mass flux however does align with the precipitation map (CO2x2 – 0.944, -1%SR – 0.872, St. Maria (NH) – 0.792, Agung (SH) – 0.935). This is likely due to the fact that convective mass flux (as done in Held and Soden (2006) and Vecchi and Soden (2007)) is estimated as $\Delta M_c/M_c = \Delta P/P - 0.07\Delta T$. As the fractional change in M_c is calculated based on precipitation directly—while ΔMSE is not, it could be expected that this metric aligns more with the modeled precipitation changes. This does however beg the question of whether moist static stability is a helpful framework to use in analyzing and diagnosing the changes in precipitation.

The fractional changes of the mass and energy balance components are summarized in Figure 8 above. As explained in the Introduction, using mass and energy balances we can approximate the change in precipitation as:

$$\frac{dP}{P} = \frac{dq}{q} + \frac{dQ}{Q} - \frac{dS}{S} + \epsilon$$

The variable *Sum* adds the fractional changes in instability (-ΔS), specific humidity (Δq), and energy (ΔQ). If our assumptions are true (and the error is low), *Sum* (dP'/P') should approximate the modeled fractional change in precipitation. However, the estimated, dP'/P', is much greater than dP/P for the non-volcanic experiments, especially in North India) and underestimates for the volcanic experiments. However, it does seem Southern India estimates of dP/P are closer than the North.

In considering the error term in our calculation of dP, one possibility is relative humidity. The calculations of dM_c/M_c, dS/S, and dP/P all assume constant relative humidity. Relative humidity is found to change slightly in the non-volcanic experiments. Especially over the semi-arid regions in the North, relative humidity increases by around 2.5% with CO2x2 and decreases by less than 2.5% with -1%SR. These fractional changes are non-negligible for the volcanic experiments and could account for some of the discrepancy.

In Southern India specifically, precipitation changes significantly even though specific humidity does not. This indicates a change in dynamics is more responsible for the precipitation changes than a thermodynamic cause. In the north, however, there are large moisture and stability changes but no major fractional changes in precipitation. Given these discrepancies in dP'/P' v. dP/P and dP/P v. dq/q or dS/S, it is clear the error term is non-negligible. There must be some other non-local mechanism(s) acting in opposition to the stability, moisture, and energy changes in the non-volcanic experiments and in concurrence the changes for the volcanic experiments (which mostly underestimate dP/P). Jacobson et al. (2020) attributes the imprecision of the stability changes to neglecting to consider horizontal advection. Bordoni and Schneider (2008) offer another possibility. They argue that the monsoons (or at least the onset) are governed largely by an interaction between tropical circulation and large-scale extratropical eddies. It also known that a subtropical jet stream exists over India and plays a role in the onset of the monsoon (Ramaswamy, 1955). Therefore, it would seem the approximation for precipitation change used in this study does not fully explain the modeled precipitation changes in India for any experiment. Further work is needed to fully explore the role of horizontal advection, eddies, and the subtropical jet on monsoon precipitation changes—particularly how these mechanisms may change under global warming and solar geoengineering.

Implications

There are some important notes to consider in interpreting the implications of these results for the real world. Firstly, it is important to note that even seemingly small precipitation changes of around 5-10% can have major consequences on agriculture, infrastructure, and human health. In fact, an all-India drought is defined as a year in which the country on average experiences more than a 10% decrease in precipitation (Kumar et al., 2013). A 5% or more shift in the mean state could shift the odds of drought. Secondly, these precipitation changes are averages. In any given year, intrinsic and natural variability—currently found to vary yearly by up to 10% of the mean value (Niranjan Kumar et al., 2013)—can make these anomalies even smaller or larger than the ones modeled here. ENSO, for instance, has been shown to affect the region (Gershunov et al. 2000; Kucharski et al. 2006) and has been linked to past droughts (Mooley and Parthasarathy, 1983; Varikoden et al., 2014).

These average changes also do not calculate changes in extreme precipitation or duration of dry spells. It is well established that mean precipitation does not increase as much as the intensity of precipitation in a warming planet (Fischer and Knutti, 2016; Myhre et al. 2019). The changes in precipitation modeled in this study do not present as each monsoon day changing by the same percentage. These changes in precipitation present themselves more as extreme rainfall events, which lead to flooding, or prolonged gaps in precipitation which lead to drought.

Another important implication is that as in Irvine et al. (2019), using solar geoengineering to offset 50% of global warming does seem to moderate the precipitation changes seen with CO2x2 over India. The two non-volcanic experiments demonstrated a high (though not perfect) negative correlation, indicating -1% SR would simply counter, and not exacerbate, the changes seen with CO2x2 (at least in India). The volcanic experiments, however, highlight the meridional component of radiative forcing. If the aerosols are injected over only one hemisphere, as found in Yang et al. (2019) and Jacobson et al. (2020), the regional consequences can be of similar magnitude to a symmetric forcing of similar or even greater magnitude. The St. Maria and Agung eruptions led to complex changes in precipitation that varied in direction (drying v. moistening) even within India. This is something to consider if solar geoengineering is ever to be utilized. If only one hemisphere begins experimentation or full-scale deployment, or if—during times of conflict or economic hardship—one hemisphere stops injections, the regional changes could be nearly as large as doubling CO_2 or blocking 1% of current solar radiation. This paper makes no claim about what should be done regarding solar geoengineering but does reveal how uneven/asymmetric deployment of aerosols could affect one region of the world which is home to nearly a billion people.

Conclusions

It was predicted that the CO2x2 and -1% experiments would largely affect identical areas within India (namely the WG and GB) while the asymmetric eruption experiments would shift the location of precipitation anomalies. It was also predicted an asymmetric forcing would lead to greater perturbations in the Indian monsoon precipitation pattern than even the CO2x2 scenario and, finally, that MSE may not prove useful in understanding the changes in precipitation, at least for the volcanic experiments.

It is found that, as predicted, the -1% solar radiation experiment decreases precipitation in a similar spatial distribution as the double CO_2 scenario increases precipitation, implying solar geoengineering—for most of India—might moderate, rather than exacerbate precipitation changes. However, the WG and GB do not prove to be the regions of greatest fractional change for precipitation, humidity, stability, convective mass flux, or energy convergence. Instead, it proves more useful to split India into subregions of North and South (along 21°N). As expected, the asymmetric, volcanic eruptions lead to more spatial discrepancies in precipitation changes, with some parts of India increasing in precipitation, while others decrease. It is also found that the Agung (SH) eruption leads to fractional precipitation changes of comparable magnitude to the double-CO_2 and -1% solar radiation experiments. These two findings suggest an uneven deployment of aerosols could be just as impactful as a doubling of CO_2 and have far less uniform consequences—even within one nation.

The mechanisms of these precipitation changes are partially explained by local changes in moist static stability, energy convergence, and specific humidity under the framework of moist static energy dynamics, but leave large residuals, indicating other non-local mechanisms like horizontal advection, eddies, and the subtropical jet stream may be important in diagnosing the causes of the precipitation changes associated with global warming and solar geoengineering.

Finally, while this paper makes no claim about what should be done regarding solar geoengineering, it does suggest that a concerted, symmetric deployment of solar geoengineering to offset half of global warming might moderate the changes expected under a double-CO_2 environment. It also highlights how an asymmetric deployment of

aerosols could lead to just as large a change in one region of the world—which is home to nearly a billion people.

References

Bal, P. K., Pathak, R., Mishra, S. K., & Sahany, S. (2019). Effects of global warming and solar geoengineering on precipitation seasonality. *Environmental Research Letters*, *14*(3), 034011. https://doi.org/10.1088/1748-9326/aafc7d

Bordoni, S., & Schneider, T. (2008). Monsoons as eddy-mediated regime transitions of the tropical overturning circulation. *Nature Geoscience*, *1*(8), 515–519. https://doi.org/10.1038/ngeo248

Chou, C., & Neelin, J. David. (2003). Mechanisms Limiting the Northward Extent of the Northern Summer Monsoons over North America, Asia, and Africa. *Journal of Climate*, *16*(3), 406–425. https://doi.org/10.1175/1520-0442(2003)016<0406:MLTNEO>2.0.CO;2

Christensen, J.H., K. Krishna Kumar, E. Aldrian, S.-I. An, I.F.A. Cavalcanti, M. de Castro, W. Dong, P. Goswami, A. Hall, J.K. Kanyanga, A. Kitoh, J. Kossin, N.-C. Lau, J. Renwick, D.B. Stephenson, S.-P. Xie and T. Zhou, 2013: Climate Phenomena and their Relevance for Future Regional Climate Change. In: Climate Change 2013: The Physical Science Basis. Contribution of Working Group I to the Fifth Assessment Report of the Intergovernmental Panel on Climate Change [Stocker, T.F., D. Qin, G.-K. Plattner, M. Tignor, S.K. Allen, J. Boschung, A. Nauels, Y. Xia, V. Bex and P.M. Midgley (eds.)]. Cambridge University Press, Cambridge, United Kingdom and New York, NY, USA

Delworth, T. L., Broccoli, A. J., Rosati, A., Stouffer, R. J., Balaji, V., Beesley, J. A., Cooke, W. F., Dixon, K. W., Dunne, J., Dunne, K. A., Durachta, J. W., Findell, K. L., Ginoux, P., Gnanadesikan, A., Gordon, C. T., Griffies, S. M., Gudgel, R., Harrison, M. J., Held, I. M., Hemler, R. S., Horowitz, L. W., Klein, S. A., Knutson, T. R., Kushner, P. J., Langenhorst, A. R., Lee, H., Lin, S., Lu, J., Malyshev, S. L., Milly, P. C. D., Ramaswamy, V., Russell, J., Schwarzkopf, M. D., Shevliakova, E., Sirutis, J. J., Spelman, M. J., Stern, W. F., Winton, M., Wittenberg, A. T., Wyman, B., Zeng, F., & Zhang, R. (2006). GFDL's CM2 Global Coupled Climate Models. Part I: Formulation and Simulation Characteristics, Journal of Climate, 19(5), 643-674. https://doi.org/10.1175/JCLI3629.1

Delworth, T. L., Rosati, A., Anderson, W., Adcroft, A. J., Balaji, V., Benson, R., Dixon, K., Griffies, S. M., Lee, H., Pacanowski, R. C., Vecchi, G. A., Wittenberg, A. T., Zeng, F., & Zhang, R. (2012). Simulated Climate and Climate Change in the GFDL CM2.5 High-Resolution Coupled Climate Model, Journal of Climate, 25(8), 2755-2781. https://doi.org/10.1175/JCLI-D-11-00316.1

Delworth, T. L., Zeng, F., Rosati, A., Vecchi, G. A., and Wittenberg, A. T. (2015). A Link between the Hiatus in Global Warming and North American Drought. Journal of Climate 28, 9, 3834-3845, doi:10.1175/JCLI-D-14-00616.1.

Fischer, E. M., & Knutti, R. (2016). Observed heavy precipitation increase confirms theory and early models. Nature Climate Change, 6(11), 986–991. https://doi.org/10.1038/nclimate3110

Gershunov, A., Schneider, N., & Barnett, T. (2001). Low-Frequency Modulation of the ENSO–Indian Monsoon Rainfall Relationship: Signal or Noise? Journal of Climate, 14(11), 2486–2492. https://doi.org/2.0.co;2">10.1175/1520-0442(2001)014<2486:lfmote>2.0.co;2

Held, I. M., and Soden, B. J. (2006). Robust Responses of the Hydrological Cycle to Global Warming. Journal of Climate 19, 21, 5686-5699, https://doi.org/10.1175/JCLI3990.1

Hijioka, Y., E. Lin, J.J. Pereira, R.T. Corlett, X. Cui, G.E. Insarov, R.D. Lasco, E. Lindgren, and A. Surjan, 2014: Asia. In: Climate Change 2014: Impacts, Adaptation, and Vulnerability. Part B: Regional Aspects. Contribution of Working Group II to the Fifth Assessment Report of the Intergovernmental Panel on Climate Change [Barros, V.R., C.B. Field, D.J. Dokken, M.D. Mastrandrea, K.J. Mach, T.E. Bilir, M. Chatterjee, K.L. Ebi, Y.O. Estrada, R.C. Genova, B. Girma, E.S. Kissel, A.N. Levy, S. MacCracken, P.R. Mastrandrea, and L.L.White (eds.)]. Cambridge University Press, Cambridge, United Kingdom and New York, NY, USA, pp. 1327-1370

Irvine, P., Emanuel, K., He, J., Horowitz, L., Vecchi, G., Keith, D. "Halving Warming with Idealized Solar Geoengineering Moderates Key Climate Hazards." *Nature Climate Change*, vol. 9, no. 4, 2019, pp. 295–299., doi:10.1038/s41558-019-0398-8.

Jacobson, T.W.P., Yang, W., Vecchi, G., Horowitz, L. "Impact of Volcanic Aerosol Hemispheric Symmetry on Sahel Rainfall." *Climate Dynamics*, vol. 55, no. 7-8, 2020, pp. 1733–1758., doi:10.1007/s00382-020-05347-7.

Jia, L., Yang, X., Vecchi, G. A., Gudgel, R. G., Delworth, T. L., Rosati, A., Stern, W. F., Wittenberg, A. T., Krishnamurthy, L., Zhang, S., Msadek, R., Kapnick, S., Underwood, S., Zeng, F., Anderson, W. G., Balaji, V., and Dixon, K. (2015). Improved Seasonal Prediction of Temperature and Precipitation over Land in a High-Resolution GFDL Climate Model. Journal of Climate 28, 5, 2044-2062, https://doi.org/10.1175/JCLI-D-14-00112.1

Knutson, T. R., & Syukuro Manabe. (1995). Time-Mean Response over the Tropical Pacific to Increased C02 in a Coupled Ocean-Atmosphere Model. *Journal of Climate*, *8*(9), 2181–2199. https://doi.org/10.1175/1520-0442(1995)008<2181:TMROTT>2.0.CO;2

Kucharski, F., Bracco, A., Yoo, J. H., & Molteni, F. (2007). Low-Frequency Variability of the Indian Monsoon–ENSO Relationship and the Tropical Atlantic: The "Weakening" of the 1980s and 1990s. Journal of Climate, 20(16), 4255–4266. https://doi.org/10.1175/jcli4254.1

Mooley, D. A., & Parthasarathy, B. (1983). Indian summer monsoon and El Nino. Pure and Applied Geophysics PAGEOPH, 121(2), 339–352. https://doi.org/10.1007/bf02590143

Myhre, G., Alterskjær, K., Stjern, C. W., Hodnebrog, Ø., Marelle, L., Samset, B. H., Sillmann, J., Schaller, N., Fischer, E., Schulz, M., & Stohl, A. (2019). Frequency of extreme precipitation increases extensively with event rareness under global warming. Scientific Reports, 9(1). https://doi.org/10.1038/s41598-019-52277-4

Niranjan Kumar, K., Rajeevan, M., Pai, D. S., Srivastava, A. K., & Preethi, B. (2013). On the observed variability of monsoon droughts over India. Weather and Climate Extremes, 1, 42–50. https://doi.org/10.1016/j.wace.2013.07.006

Ramaswamy, C. (1956) On the Sub-tropical Jet Stream and its Role in the Development of Large-scale Convection, Tellus, 8:1, 26-60, DOI: 10.3402/tellusa.v8i1.8943

Robock, A. (2008). 20 reasons why geoengineering may be a bad idea. Bulletin of the Atomic Scientists, 64(2), 14–18. https://doi.org/10.2968/064002006
Robock, A. (2015). Chapter 53—Climatic impacts of volcanic eruptions. In H. Sigurdsson (Ed.), The encyclopedia of volcanoes (2nd ed., pp.935–942). Amsterdam: Academic Press. https://doi.org/10.1016/B978-0-12-385938-9.00053-5
Sahany, S., Mishra, S. K., Pathak, R., & Rajagopalan, B. (2018). Spatiotemporal variability of seasonality of rainfall over India. Geophysical Research Letters, 45, 7140–7147. https://doi.org/10.1029/2018GL077932
Seth, A., Rauscher, S. A., Biasutti, M., Giannini, A., Camargo, S. J., & Rojas, M. (2013). CMIP5 Projected Changes in the Annual Cycle of Precipitation in Monsoon Regions. *Journal of Climate*, *26*(19), 7328–7351. https://doi.org/10.1175/jcli-d-12-00726.1
United Nations Framework Convention on Climate Change. (2021). *Nationally determined contributions under the Paris Agreement. Synthesis report by the secretariat.* (Report No.: FCCC/PA/CMA/2021/2), available from: https://unfccc.int/documents/268571
Varikoden, H., Revadekar, J. V., Choudhary, Y., & Preethi, B. (2014). Droughts of Indian summer monsoon associated with El Niño and Non-El Niño years. International Journal of Climatology, 35(8), 1916–1925. https://doi.org/10.1002/joc.4097
Vecchi, G. A., Delworth, T., Gudgel, R., Kapnick, S., Rosati, A., Wittenberg, A. T., Zeng, F., Anderson, W., Balaji, V., Dixon, K., Jia, L., Kim, H.-S., Krishnamurthy, L., Msadek, R., Stern, W. F., Underwood, S. D., Villarini, G., Yang, X., & Zhang, S. (2014). On the Seasonal Forecasting of Regional Tropical Cyclone Activity, Journal of Climate, 27(21), 7994-8016., https://doi.org/10.1175/JCLI-D-14-00158.1
Vecchi, G.A. and Harrison, D.E. (2004). Interannual Indian Rainfall Variability and Indian Ocean Sea Surface Temperature Anomalies. In Earth's Climate (eds C. Wang, S. Xie and J. Carton). https://doi.org/10.1029/147GM14
Vecchi, G. A., and Soden, B. J. (2007). Global Warming and the Weakening of the Tropical Circulation. Journal of Climate 20, 17, 4316-4340, https://doi.org/10.1175/JCLI4258.1
Yang, W., Vecchi, G., Fueglistaler, S., Horowitz, L. W., Luet, D. J., Muñoz, Á. G., et al. (2019). “Climate Impacts from Large Volcanic Eruptions in a High-Resolution Climate Model: The Importance of Forcing Structure.” *Geophysical Research Letters*, vol. 46, no. 13, 2019, pp. 7690–7699., doi:10.1029/2019gl082367.
Yang, X., Vecchi, G. A., Gudgel, R. G., Delworth, T. L., Zhang, S., Rosati, A., Jia, L., Stern, W. F., Wittenberg, A. T., Kapnick, S., Msadek, R., Underwood, S. D., Zeng, F., Anderson, W., and Balaji, V. (2015). Seasonal Predictability of Extratropical Storm Tracks in GFDL’s High-Resolution Climate Prediction Model. Journal of Climate 28, 9, 3592-361, https://doi.org/10.1175/JCLI-D-14-00517.1
Zhou, C., Zelinka, M. D., Dessler, A. E., & Wang, M. (2021). Greater committed warming after accounting for the pattern effect. Nature Climate Change, 11(2), 132–136. https://doi.org/10.1038/s41558-020-00955-x